Submitted to *Materials Characterization*, October, 2018

Revised January, 2019

(MATERIALSCHAR_2018_2711)

Effects of initial {10-12} twins on cyclic deformation and fatigue of magnesium alloy at low strain amplitudes

Fenghua Wang[1], Man Liu[1], Jie Sun[1], Miaolin Feng[2], Li Jin[1], Jie Dong[1*], Yanyao Jiang[3]

[1] National Engineering Research Center of Light Alloy Net Forming & State Key Laboratory of Metal Matrix Composites, Shanghai Jiao Tong University, Shanghai 200240, China

Phone: 021-34203052, Fax: 021-34202794, E-mail: jiedong@sjtu.edu.cn

[2] Department of Engineering Mechanics, Shanghai Jiao Tong University, Shanghai 200240, China

[3] Department of Mechanical Engineering, University of Nevada, Reno, NV89557, USA

Abstract: An extruded AZ31B (Mg-3Al-1Zn-0.5Mn) magnesium alloy with a twin volume fraction of 60% was subjected to fully reversed strain-controlled tension-compression along the extrusion direction at strain amplitudes ranging from 0.23% to 0.45%. Dislocation slips were the dominant plastic deformation mechanisms without involving persistent twinning-detwinning. At an identical strain amplitude, the fatigue life of the pre-twinned alloy was much lower than that of the as-extruded alloy. Fatigue cracks were mainly initiated on the prismatic or prismatic-basal slip bands in the parent grains. The material volume reduction of the parent grains in the pre-twinned alloy enhanced fatigue damage. Twin cracks were not observed.

Keywords: Magnesium alloy; {10-12} extension twin; Cyclic deformation; Fatigue damage; Persistent slip band

1. Introduction

Wrought magnesium (Mg) alloys have been increasingly applied in engineering due to their low density and high specific strength [1, 2]. The cyclic deformation and fatigue of wrought Mg alloys such as AZ31B [3-5], AM30 [6-8], ZK60A [9-12], GW83 [13] have been investigated. These studies reveal that the deformation and damage mechanisms of low cycle fatigue in Mg alloys are related to a distinguishable kink point in the strain-fatigue life curves. When the strain amplitudes are lower than the kink point, dislocation slips were the dominant plastic deformation mechanism and fully symmetric stress-strain hysteresis loops were observed [14, 15]. Fatigue cracks are found to initiate at the persistent slip bands (PSBs) [16-18] and the grain boundaries (GBs) [19], and the final failure is due to continuous accumulation of distributed microcracks. When the strain amplitudes are higher than the kink point, sustainable twinning-detwinning occurs and the materials exhibit typical sigmoidal shaped stress-strain hysteresis loops. Fatigue cracks are mainly initiated at the GBs [19] and the twin boundaries (TBs) [20, 21], and the fatigue failure is a result of continuous crack initiation and microcrack coalescence.

Extension twinning {10-12} plays an important role in the deformation behavior of Mg alloys. It introduces a crystallographic lattice rotation of 86.3° and the lattice of the twinned region is favored for detwinning under subsequent reversed loading [22]. Park et al. [23, 24] reported that at a strain amplitude of 1.0%, pre-existing {10-12} twins in a rolled AZ31B alloy caused an increase in the mean stress under cyclic loading, which deteriorated the fatigue resistance. However, little work has been done on the effect of pre-existing twins on the fatigue property in wrought Mg alloys at strain amplitudes lower than the kink point. Loading amplitudes lower than that of the kink point in the strain-life curve is referred to as “low strain amplitude” in the current presentation. At low strain amplitudes, most of the twins formed before the fatigue experiments would be unchanged during the fatigue loading. In the current study, cyclic deformation and fatigue of an AZ31B alloy with an initial {10-12} twin volume fraction of 60% were experimentally investigated by fully reversed strain-controlled tension-compression along the extrusion direction (ED). Particularly, fatigue damage

evolution through a surface crack observation on an ex situ sample was studied at a strain amplitude of 0.3%.

2. Materials and Experiments

An extruded round rod with a nominal composition Mg-3Al-Zn-0.5Mn (wt%) was compressed to a strain of 6.0% along the ED followed by annealing at 260°C for 15 minutes and quenched in water at room temperature in order to eliminate deformation dislocations and to release the residual stresses. A longer annealing time would induce precipitations. All the testing specimens for monotonic and cyclic experiments were cut from the rod having a diameter of 76mm (Figure 1a). The plate specimens were distributed along the outer surface of the round rod with their axes parallel to the extrusion direction of the material. An electron back-scattered diffraction (EBSD) examination revealed approximate 60% volume fraction of {10-12}<10-11> twins after 6% compression. A surface scan using scanning electron microscopy (SEM) indicated that there were no cracks induced by the pre-compression. Fig. 1b shows the inverse pole figure (IPF) map of the pre-twinned AZ31B alloy on the ED-RD plane before fatigue experiments. The parent grains have their <0001> directions perpendicular to ED (red color) while numerous {10-12}<10-11> tension twins have their <0001> directions almost parallel to the ED (green or blue color). The twins divided the grains into smaller and irregular shaped fragments.

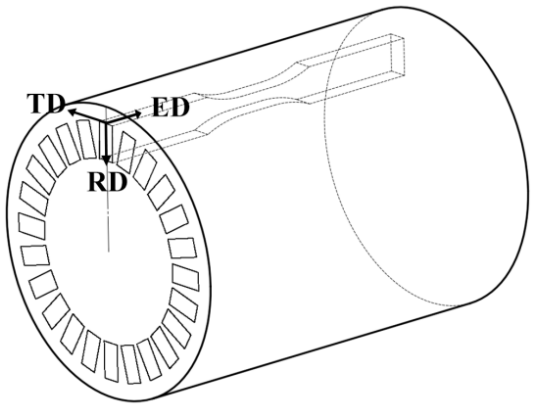

(a)

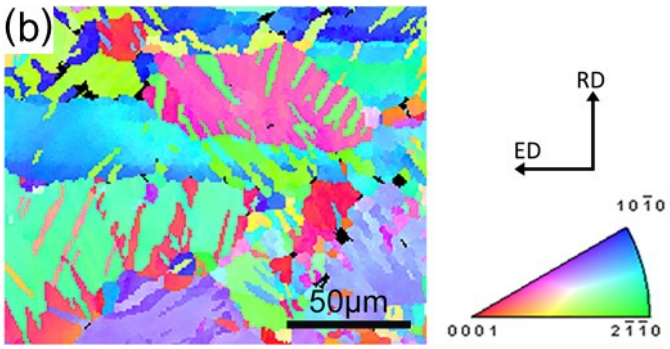

Fig. 1. (a) Schematic of the testing specimens of as-extruded and pre-twinned AZ31B alloys. ED-extrusion direction, RD-radial direction, TD-transverse direction. (b) Inverse pole figure of pre-twinned AZ31B alloy obtained by EBSD.

Detailed sample preparation procedure, fatigue equipment, and environment were described in Ref. [25]. Fully reversed strain-controlled tension-compression fatigue tests were conducted at room temperature with the strain amplitudes ranging from 0.23% to 0.45% at a loading frequency of 10 Hz. The twin-free extruded AZ31B alloy was also tested at identical strain amplitudes for a comparison of results. In order to facilitate discussions, the extruded alloy without pre-strain will be referred to as as-extruded alloy while the AZ31B alloy after 6% compression strain will be called pre-twinned alloy. Fatigue life of a testing specimen was defined as the moment when the tensile peak stress was decreased by 10% from the highest peak value. For a fatigue specimen tested at a strain amplitude of 0.3%, SEM observations were performed at 1500th, 3000th, 6000th, 12000th, 18000th and 22000th (~95% fatigue life) loading cycles and microstructures were examined by EBSD at 6000th and 12000th loading cycles. In order to investigate the fatigue damage development, the ED-RD surface of the plate specimen was preetched prior to the fatigue experiment using the same procedure as that used for optical microscopy (OM) and SEM. Grain boundaries (GBs) and twin boundaries (TBs) were revealed by soaking the polished samples in an Acetic-Etchant solution of 1g oxalic acid, 1ml nitric acid, 1ml acetic acid and 150ml distilled water for 10 seconds. The ED-RD surface of the sample for EBSD observation was mechanically polished and chemically preetched by an Acetic-Nitric solution of 5ml nitric acid, 15ml acetic acid, 20ml water, and 60ml ethanol for 1~2 s.

3. Results and Discussion

3.1 Cyclic deformation of as-extruded and pre-twinned AZ31B alloys

Figure 2a shows the stress-plastic strain hysteresis loops of the pre-twinned material and these of the as-extruded state at a strain amplitude of 0.3%. With a twin-free initial state, the as-extruded AZ31B alloy loaded in the ED exhibits symmetric stress-strain hysteresis loops at strain amplitudes below 0.45% [14, 15, 25, 26]. For the pre-twinned alloy, the stress-strain hysteresis loops evolve from a near symmetric shape in the first 20 cycles to a fully symmetric shape eventually. Such a transition in the stress-strain hysteresis loops reflects limited twinning-detwinning activities in the early loading cycles and a lack of sustainable twinning-detwinning after a certain number of loading cycles [27, 28]. Fig. 2b shows stress-plastic strain hysteresis loops at half-life cycles of pre-twinned AZ31B alloy. The stabilized hysteresis loops are almost fully symmetric when strain amplitude is lower than 0.45%. As a result, most of the twins formed before the fatigue experiments were unchanged during the fatigue loading. Similar to the as-extruded alloy, the peak stresses of pre-twinned alloy experienced marginal cyclic hardening, which could be ascribed to dislocation immobilization by the twin boundaries and activation of non-basal slips [29, 30].

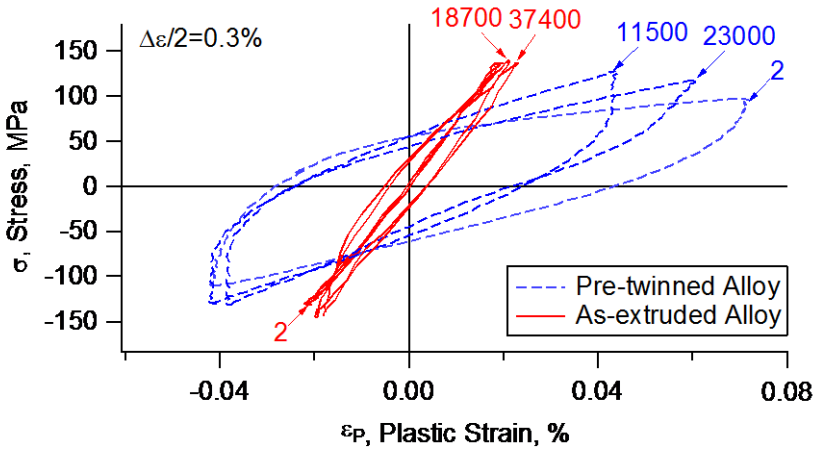

(a)

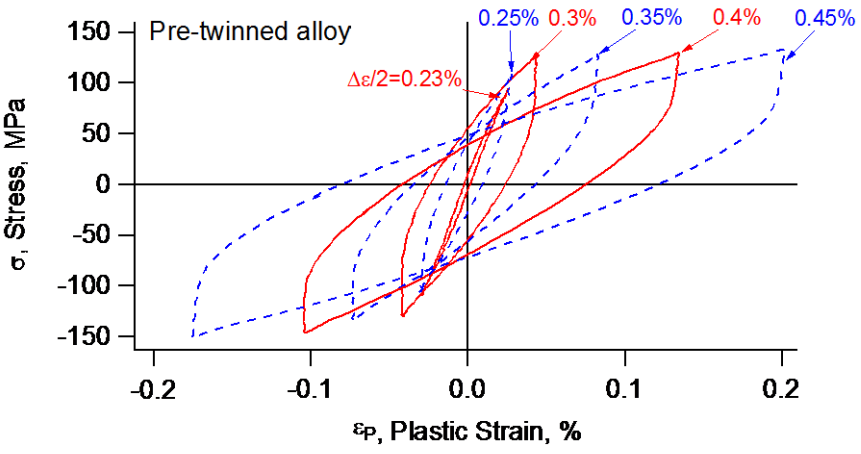

(b)

Fig. 2. (a) Stress-plastic strain hysteresis loops at a strain amplitude of 0.3% of as-extruded and pre-twinned AZ31B alloy, (b) Stress-Plastic strain hysteresis loops at half-life cycles of pre-twinned AZ31B alloy.

Fatigue results of as-extruded and pre-twinned AZ31B alloys are summarized in Table 1. The stress values listed in Table 1 were obtained at approximately half fatigue lives. The strain-fatigue life curves are shown in Fig. 3a. It can be found that at an identical strain amplitude, the fatigue life of the pre-twinned alloy was much shorter than that of the as-extruded alloy. Due to the existence of twins, the fully reversed strain-controlled fatigue experiments of the pre-twinned alloy displayed small compressive mean stresses. Since a tensile mean stress usually enhances fatigue damage, the results shown in Table 1 and Fig. 3a suggest that the mean stress does not contribute to the observed higher fatigue life of the extruded alloy than that of the pre-twinned alloy at an identical strain amplitude. Fig. 3b shows the curves of the plastic strain energy density per loading cycle and fatigue life for the two alloys. It turns out that the relationship between the plastic strain energy density per loading cycle and fatigue life is practically identical for as-extruded and pre-twinned conditions.

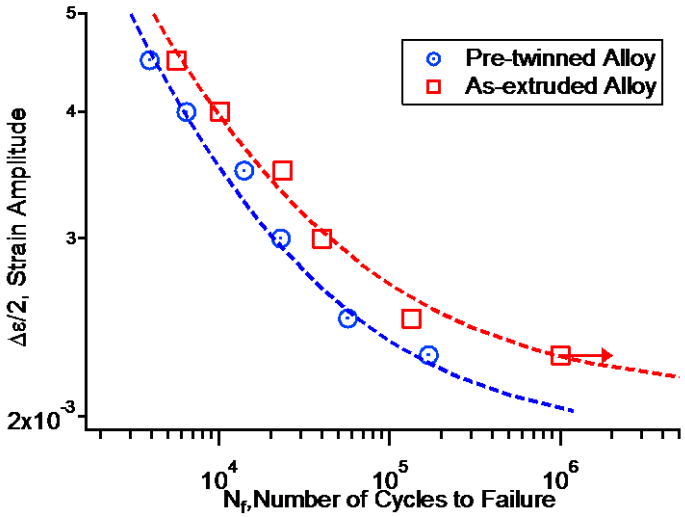

(a)

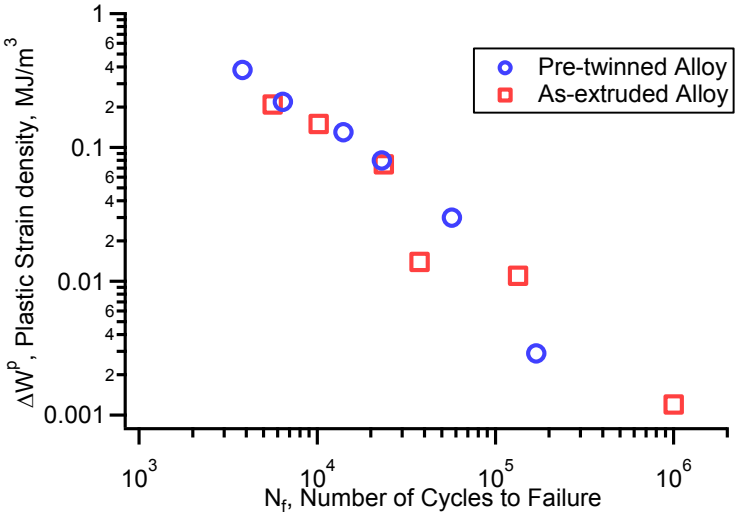

(b)

Fig. 3. (a) Strain-life curves, (b) Plastic strain energy density per loading cycle and fatigue life of pre-twinned and as-extruded AZ31B alloys.

Table1 Fatigue results of as-extruded and pre-twinned AZ31B alloy

Alloy	ID	Δε/2(%)	Δσ/2(MPa)	σ_m(MPa)	ΔW^p(MJ/m^3)	N_f
	31E1	0.45	161.7	17.1	0.21	5,620
	31E2	0.40	150.4	13.5	0.15	10,168
As-	31E3	0.35	134.4	1.6	0.075	23,600
extruded	31E4	0.30	142.2	4.1	0.014	37,400
	31E5	0.25	110.2	-3.8	0.011	133,500
	31E6	0.23	104.0	-0.2	0.0012	＞1,000,000

	31T1	0.45	142.2	-9.6	0.38	3,800
	31T2	0.40	137.9	-9.6	0.22	6,400
Pre-	31T3	0.35	130.9	-3.4	0.13	14,000
twinned	31T4	0.30	128.8	-1.3	0.08	23,000
	31T5	0.25	108.3	-0.2	0.03	56,800
	31T6	0.23	101.2	0.3	0.0029	169,200

Notes: $\Delta\varepsilon/2$-strain amplitude; $\Delta\sigma/2$-stress amplitude at half-life cycle; σ_m-mean stress at half-life cycle; ΔW^p-plastic strain energy density per loading cycle at half-fatigue life; N_f-number of cycles to failure.

3.2 Fatigue damage of pre-twinned AZ31B alloy

Figure 4 presents the ex situ SEM observations of the surface damage morphology from 6000th to 22000th loading cycles in the same area of the pre-twinned AZ31B alloy at a strain amplitude of 0.3%. Several microcracks were first detected at 3000th loading cycle in an observation area of 5 mm ×10 mm. As a comparison, initiation started much later in the as-extruded alloy at an identical strain amplitude [25]. With increasing loading cycles, the total number of fatigue cracks increased. More than 10 microcracks were identified at 6000th cycle (Fig. 4a). These microcracks were divided into two types, as shown in Fig. 4b and 4c. One type of cracks had an angle of ~53° from the horizontal axis and the extrusions and intrusions were parallel and were located in a narrow band of the matrix. The other type of cracks made an angle of ~62° from the horizontal axis and the extrusions and intrusions were intersected in the matrix. Fig. 4d and 4e show the surface morphology at 12000th and 22000th cycles, respectively. With increasing loading cycles, much more persistent slip band (PSB) cracks appeared from 12000th cycle to near fatigue failure. The increase in the length and width of the microcracks was insignificant. PSBs and cracks at high magnification are presented in Fig. 4f. It was noticed the cracks shown in Fig. 4f remained the initial morphology in Fig. 4b and 4c. Few twin cracks, twin boundary cracks or grain boundary cracks were detected and they remained unchanged.

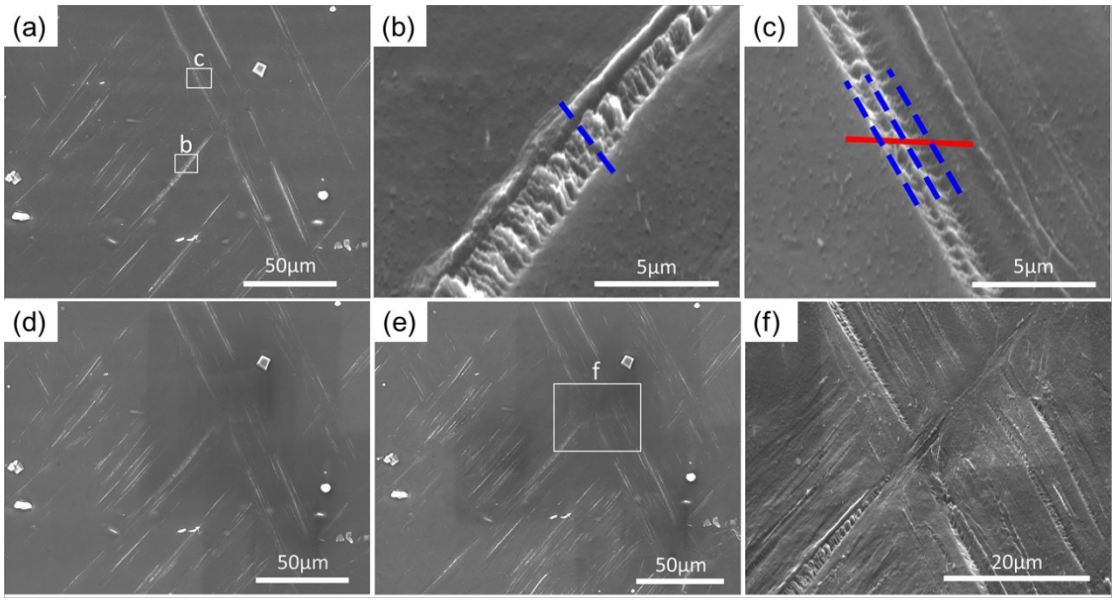

Fig. 4. Ex situ SEM micrographs of surface damages at a strain amplitude of 0.3%: (a) at 6000th cycle, (b) high magnification of PSBs in (a), (c) high magnification of PSBs in (a), (d) at 12000th cycle, (e) at 22000th cycle, (f) high magnification of PSBs and cracks (loading along the horizontal direction).

Figure5a and 5b show the distribution of Schmid factor (SF) values of basal slips and prismatic slips in twins and parent grains. Fig. 5a shows that the SF values of the prismatic slip in most of twins are lower than 0.1, which is much lower than that of basal slip. It can be speculated that basal slips with lower critical resolved shear stress (CRSS) were the dominant slip mechanism in the twins. In parent grains, the SF values of the basal slips in approximately 40% grains are less than 0.1, while these for the prismatic slips in more than 97% grains are greater than 0.4. According to the visco plastic self-consistent (VPSC) simulation, the CRSS for basal slip, prismatic slip, pyramidal slip, and extension twin are 15 MPa, 60 MPa, 90 MPa and 23 MPa, respectively [31, 32]. Therefore, both basal slip and prismatic slip can occur in the parent grains during cyclic deformation.

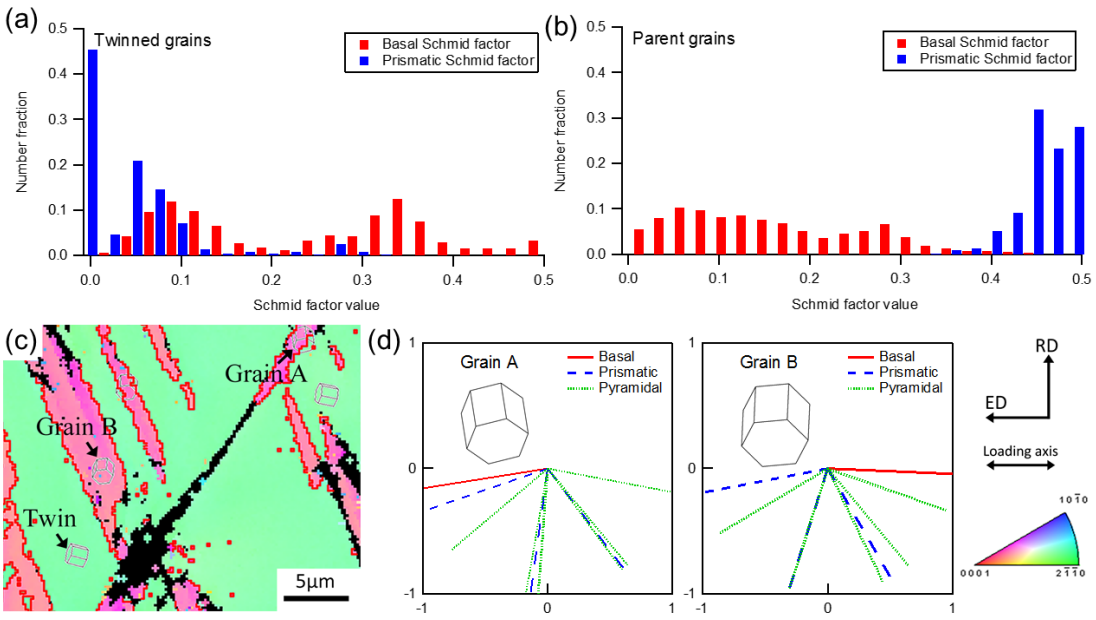

Fig. 5. Distribution of Schmid factor values of basal slip and prismatic slip of (a) twinned grains and (b) parent grains, (c) Inverse pole figure map at a strain amplitude of 0.3% at 6000th cycle, (d) Slip system selection for Grain A and Grain B (codes 1-12 corresponding to the slip system numbers, loading along the horizontal direction).

Figure 5c displays the IPF map of the surface damage morphology at 6000th loading cycle at a strain amplitude of 0.3%. The two parent grains marked as Grain A and Grain B, corresponded to these in Fig. 4b and 4c. The maximum SF values of the basal slips and prismatic slips are 0.11 and 0.49 for Grain A and Grain B, respectively. The possible slip traces of the two grains are presented in Fig. 5d. The x- and y-axes are dimensionless representing the same directions as those in Fig. 4. One set of slip traces matches one slip system [19]. The PSBs in Grain A are parallel to (10-10)[11-20] prismatic slip traces. It is obvious that these PSBs in Grain A were resulted from (10-10)[11-20] prismatic slip. In addition, the two series of PSBs in Grain B are parallel to (0001)[-2110] basal slip traces and (10-10)[11-20] prismatic slip traces, respectively. It can be inferred that these PSBs in Grain B are due to (0001)[-2110] basal slip and (10-10)[11-20] prismatic slip. In other words, prismatic slip is more likely to cause fatigue microcracks than basal slip since the former is favorable for the formation of microcracks in the parent grains.

Xiong et al. [33] reported the effect of material orientation on cyclic deformation and fatigue behavior of rolled AZ80 alloy. The fatigue life of the rolled direction (RD) specimen was the longest at a strain amplitude below 0.4%, and the normal direction (ND) specimen had the lowest fatigue resistance. The RD and ND specimens are similar to the loading along the extrusion and radial directions, respectively. Based on the experimental observations of surface damage morphology at a low strain amplitude, proposed microcrack initiation modes in the extruded alloy are illustrated in Fig. 6. When the as-extruded specimens are loaded along extrusion direction (Fig. 6a), prismatic slip and basal slip are likely to occur in some favorably orientated grains. When the specimen is loaded in the radial direction (Fig. 6b), basal slip is easiest to activate, which is similar to the deformation mechanisms in the twins. Fig. 6c shows that the crystal reorientation is a result of tension twinning. Prismatic slip and basal slip are predominant deformation modes in the parent grains and twinned grain, respectively. Once the prismatic slip exceeds the critical dislocation density, the PSB crack is prior to appear in the surface. It is difficult to capture the slip trace and PSB crack in the twins. Moreover, the abrupt strain relaxation due to twinning effectively hinders nucleation of new microcracks in twins [10, 16, 34, 35]. The initial deformation twins produce no obvious and direct changes in fatigue damage at low strain amplitudes [36, 37]. As for the pre-twinned alloy subjected to loading along extrusion direction, the reduced material volume of the parent grains due to twinning may cause the crack initiation life to decrease. Considering crack initiation usually takes up more than 90% of the total fatigue life at low strain amplitudes, the fatigue life of the pre-twinned alloy is shorter than that of as-extruded alloy.

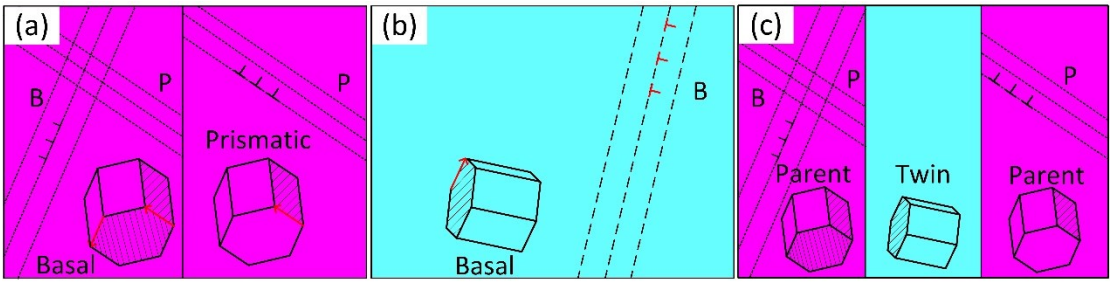

Fig. 6. Schematics of the proposed microcrack initiation modes in the extruded alloy: loading

direction along (a) extrusion direction; (b) radial direction; and (c) extrusion direction for pre-twinned alloy (loading along the horizontal direction, B-basal plane, P-prismatic plane).

4. Conclusions

The effects of initial {10-12} twins on the cyclic deformation and fatigue damage of an AZ31B alloy were experimentally studied. At slip-dominated strain amplitudes varying from 0.23% to 0.45%, the stress-strain hysteresis loops displayed a symmetrical shape after several loading cycles. The fatigue life of the pre-twinned material was much shorter than that of the as-extruded state at an identical strain amplitude. The PSB cracks were incessantly initiated during cyclic loading that leads to final fatigue failure. Fatigue damage was enhanced due to the volume reduction of the parent grains in the pre-twinned alloy. Twin cracks were seldom observed.

Acknowledgements

Fenghua Wang and Jie Dong gratefully acknowledge the support of the National Key Research and Development Program of China (2016YFB0101604), National Natural Science Foundation of China (51601112), Shanghai Rising-Star Program (17QB1403000). Miaolin Feng thanks support by National Natural Science Foundation of China (11572191). Yanyao Jiang thanks support from the National Science Foundation (CMMI-1762312).

References

[1] V.V. Ogarevic, R.I. Stephens, Fatigue of Magnesium Alloys, Annu. Rev. Mater. Sci. 20 (1990) 141-177.

[2] I.J. Polmear, Magnesium alloys and applications, Mater. Sci. Technol. 10 (1994) 1-16.

[3] X.Z. Lin, D.L. Chen, Strain controlled cyclic deformation behavior of an extruded magnesium alloy, Mater. Sci. Eng. A 496 (2008) 106-113.

[4] Y. Xiong, Q. Yu, Y. Jiang, Multiaxial fatigue of extruded AZ31B magnesium alloy, Mater. Sci. Eng. A 546 (2012) 119-128.

[5] D. Toscano, S.K. Shaha, B. Behravesh, H. Jahed, B. Williams, Effect of forging on the low cycle fatigue behavior of cast AZ31B alloy, Mater. Sci. Eng. A 706 (2017) 342–356.

[6] C.L. Fan, D.L. Chen, A.A. Luo, Dependence of the distribution of deformation twins on strain

amplitudes in an extruded magnesium alloy after cyclic deformation, Mater. Sci. Eng. A 519 (2009) 38-45.
[7] T.J. Luo, Y.S. Yang, W.H. Tong, Q.Q. Duan, X.G. Dong, Fatigue deformation characteristic of as-extruded AM30 magnesium alloy, Mater. Des. 31 (2010) 1617-1621.
[8] A.A. Roostaei, H. Jahed, Role of loading direction on cyclic behaviour characteristics of AM30 extrusion and its fatigue damage modelling, Mater. Sci. Eng. A, 670 (2016) 26-40.
[9] L. Wu, A. Jain, D.W. Brown, G.M. Stoica, S.R. Agnew, B. Clausen, D.E. Fielden, P.K. Liaw, Twinning-detwinning behavior during the strain-controlled low-cycle fatigue testing of a wrought magnesium alloy, ZK60A, Acta Mater. 56 (2008) 688-695.
[10] L. Wu, S.R. Agnew, D.W. Brown, G.M. Stoica, B. Clausen, A. Jain, D.E. Fielden, P.K. Liaw, Internal stress relaxation and load redistribution during the twinning-detwinning-dominated cyclic deformation of a wrought magnesium alloy, ZK60A, Acta Mater. 56 (2008) 3699-3707.
[11] Q. Yu, J. Zhang, Y. Jiang, Q. Li, An experimental study on cyclic deformation and fatigue of extruded ZK60 magnesium alloy, Int. J. Fatigue 36 (2012) 47-58.
[12] A.H. Pahlevanpour, S.M.H. Karparvarfard, S.K. Shaha, S.B. Behravesh, S. Adibnazari, H. Jahed, Anisotropy in the quasi-static and cyclic behavior of ZK60 extrusion: Characterization and fatigue modeling, Mater. Des. 160 (2018) 936-948.
[13] F. Wang, J. Dong, Y. Jiang, W. Ding, Cyclic deformation and fatigue of extruded Mg-Gd-Y magnesium alloy, Mater. Sci. Eng. A 561 (2013) 403-410.
[14] M. Matsuzuki, S. Horibe, Analysis of fatigue damage process in magnesium alloy AZ31, Mater. Sci. Eng. A 504 (2009) 169-174.
[15] X. Lou, M. Li, R. Boger, S. Agnew, R. Wagoner, Hardening evolution of AZ31B Mg sheet, Int. J. Plast. 23 (2007) 44-86.
[16] P. Lukáš, L. Kunz, Role of persistent slip bands in fatigue, Philos. Mag. 84 (2004) 317-330.
[17] J.D. Bernard, J.B. Jordon, M.F. Horstemeyer, H.E. Kadiri, J. Baird, D. Lamb, A.A. Luo, Structure-property relations of cyclic damage in a wrought magnesium alloy, Scripta Mater. 63 (2010) 751-756.
[18] K. Gall, G. Biallas, H.J. Maier, P. Gullett, M.F. Horstemeyer, D.L. McDowell, J. Fan, In-situ observations of high cycle fatigue mechanisms in cast AM60B magnesium in vacuum and water vapor environments, Int. J. Fatigue 26 (2004) 59-70.
[19] F. Wang, J. Dong, M. Feng, J. Sun, W. Ding, Y. Jiang, A study of fatigue damage development in extruded Mg-Gd-Y magnesium alloy, Mater. Sci. Eng. A 589 (2014) 209-216.
[20] S.H. Park, S.-G. Hong, J.-H. Lee, S.-H. Kim, Y.-R. Cho, J. Yoon, C.S. Lee, Effects of pre-tension on fatigue behavior of rolled magnesium alloy, Mater. Sci. Eng. A 680 (2017) 351-358.
[21] F. Yang, S.M. Yin, S.X. Li, Z.F. Zhang, Crack initiation mechanism of extruded AZ31 magnesium alloy in the very high cycle fatigue regime, Mater. Sci. Eng. A 491 (2008) 131-136.
[22] Q. Yu, J. Zhang, Y. Jiang, Q. Li, Effect of strain ratio on cyclic deformation and fatigue of extruded AZ61A magnesium alloy, Int. J. Fatigue 44 (2012) 225-233.
[23] S.H. Park, S.-G. Hong, C.S. Lee, Role of initial {1 0-1 2} twin in the fatigue behavior of rolled Mg-3Al-1Zn alloy, Scripta Mater. 62 (2010) 666-669.
[24] S.H. Park, Effect of initial twins on the stress-controlled fatigue behavior of rolled magnesium alloy, Mater. Sci. Eng. A 680 (2017) 214-220.
[25] B. Wen, F. Wang, L. Jin, J. Dong, Fatigue damage development in extruded Mg-3Al-Zn magnesium alloy, Mater. Sci. Eng. A 667 (2016) 171-178.

[26] Y. Xiong, Q. Yu, Y. Jiang, Cyclic deformation and fatigue of extruded AZ31B magnesium alloy under different strain ratios, Mater. Sci. Eng. A 649 (2016) 93-103.
[27] D. Hou, T. Liu, L. Luo, L. Lu, H. Chen, D. Shi, Twinning behaviors of a rolled AZ31 magnesium alloy under multidirectional loading, Mater. Charact. 124 (2017) 122-128.
[28] S. Dong, Q. Yu, Y. Jiang, J. Dong, F. Wang, L. Jin, W. Ding, Characteristic cyclic plastic deformation in ZK60 magnesium alloy, Int. J. Plast. 91 (2017) 25-47.
[29] Q. Yu, Y. Jiang, J. Wang, Cyclic deformation and fatigue damage in single-crystal magnesium under fully reversed strain-controlled tension-compression in the [100] direction, Scripta Mater. 96 (2015) 41-44.
[30] H. Wang, P.D. Wu, J. Wang, Modeling inelastic behavior of magnesium alloys during cyclic loading-unloading, Int. J. Plast. 47 (2013) 49-64.
[31] S.R. Agnew, C.N. Tomé, D.W. Brown, T.M. Holden, S.C. Vogel, Study of slip mechanisms in a magnesium alloy by neutron diffraction and modeling, Scripta Mater. 48 (2003) 1003-1008.
[32] A. Styczynski, C. Hartig, J. Bohlen, D. Letzig, Cold rolling textures in AZ31 wrought magnesium alloy, Scripta Mater. 50 (2004) 943-947.
[33] Y. Xiong, Y. Jiang, Cyclic deformation and fatigue of rolled AZ80 magnesium alloy along different material orientations, Mater. Sci. Eng. A 677 (2016) 58-67.
[34] B. Clausen, C.N. Tomé, D.W. Brown, S.R. Agnew, Reorientation and stress relaxation due to twinning: Modeling and experimental characterization for Mg, Acta Mater. 56 (2008) 2456-2468.
[35] O. Muránsky, D.G. Carr, P. Šittner, E.C. Oliver, In situ neutron diffraction investigation of deformation twinning and pseudoelastic-like behaviour of extruded AZ31 magnesium alloy, Int. J. Plast 25 (2009) 1107-1127.
[36] J. Koike, N. Fujiyama, D. Ando, Y. Sutou, Roles of deformation twinning and dislocation slip in the fatigue failure mechanism of AZ31 Mg alloys, Scripta Mater. 63 (2010) 747-750.
[37] D.K. Xu, L. Liu, Y.B. Xu, E.H. Han, The crack initiation mechanism of the forged Mg-Zn-Y-Zr alloy in the super-long fatigue life regime, Scripta Mater. 56 (2007) 1-4.